

Nonlinear charge injection in organic field-effect transistors

B.H. Hamadani and D. Natelson

Department of Physics and Astronomy, Rice University, 6100 Main St., Houston, TX 77005

(Dated: February 8, 2020)

Transport properties of a series of poly(3-hexylthiophene) organic field effect transistors with Cr, Cu and Au source/drain electrodes were examined over a broad temperature range. The current-voltage characteristics of the injecting contacts are extracted from the dependence of conductance on channel length. With reasonable parameters, a model of hopping injection into a disordered density of localized states, with emphasis on the primary injection event, agrees well with the field and the temperature dependence of the data over a broad range of temperatures and gate voltages.

PACS numbers:

I. INTRODUCTION

Field effect transistors based on organic semiconductors (OFETs) have attracted interest for their potential applications as inexpensive and flexible electronics[1]. The physics of charge injection at the metal-organic semiconductor (OSC) contact in such field-effect devices remains poorly understood. Contact resistance is often neglected when inferring the mobility from transistor transport characteristics. It is known, however, that the parasitic series resistance, R_s , at the OSC-metal interface can play an important role[2]. Several experiments have already shown that it can easily dominate the intrinsic channel resistance, R_{ch} , in short channel (few microns and below) devices[3, 4, 5]. Approaches used to differentiate between contact and channel resistances include analyses of single device characteristics[6, 7], scanning potentiometry[8, 9, 10], and scaling of total device resistance with channel length in a series of devices[3, 4, 5, 11, 12, 13].

In a previous study[5], we reported measurements of R_s and the true channel resistance in bottom contact poly(3-hexylthiophene) (P3HT) field effect transistors as a function of temperature. In that study, which used Au source and the drain electrodes, we found that R_s correlates inversely with mobility over four decades, over a broad range of temperatures and gate voltages. This is consistent with the predictions of a recent theory[14, 15] of OSC-metal contacts incorporating a thermionic emission model with diffusion-limited injection currents and accounting for the backflow of charge at the interface. Such a model predicts an inverse relationship between the mobility and the contact resistivity, provided that the Schottky barrier between Au and P3HT is low. This is expected to be the case since the highest occupied molecular orbital (HOMO) of P3HT is estimated[16] to lie between 5.1 and 5.2 eV, close to the work function of Au (5.2 eV)[10].

In the case of lower work function metals such as Cr and Cu (~ 4.7 eV) [10], a significant Schottky energy barrier, Δ , for holes is expected to exist at the OSC-metal interface. For a channel mobility, μ , that is thermally activated with characteristic energy E_a , typically $< \sim 0.1$ eV, the same model predicts a temperature dependence of

the contact resistance[5], $R_s \propto \exp([E_a + \Delta]/k_B T)$. For $\Delta \sim 0.3$ eV, the temperature dependence of R_s is therefore predicted to be much stronger than the Au electrode case. However, in recent studies of charge injection in both bottom-contact P3HT field effect transistors[10] and hole injection from an Ag electrode into polydialkoxy-p-phenylene vinylene[17], only a weak temperature dependence of contact resistance or injecting current was observed. These results imply that the diffusion-limited thermionic emission model is inadequate.

In this work, we examine this issue through the temperature and field dependence of charge injection in bottom contact OFETs based on P3HT with different source/drain electrode materials. To differentiate between the current-voltage characteristics of the channel and the contacts, we examine the scaling of device current with channel length, employ the gradual channel approximation[7], and divide the total source-drain voltage V_D into a channel component and a voltage dropped at the contacts, V_C . We assume, as supported by scanning potentiometry[10], that V_C is dominantly dropped at the injecting contact for metals with a significant Δ . We use $I_D - V_D$ data from a given series of devices of varying channel length, L , and fixed width, W , to extract both μ and $I_D - V_C$ for this OSC/metal interface. As expected, the $I_D - V_C$ characteristics of a specific OSC/metal interface are unique at a given temperature and gate voltage, independent of L . We analyze the field and temperature dependence of the injected current through a recent analytical model[18] of charge injection from a metallic electrode into a random hopping system. With reasonable fit parameters, this model agrees well with the observed temperature and field dependence of the injected current. We also discuss the distance scale over which V_C is dropped, and further experimental avenues to explore.

II. EXPERIMENTAL DETAILS

Devices are made in a bottom contact configuration[5] on a degenerately doped $p+$ silicon substrate used as a gate. The gate dielectric is 200 nm of thermal SiO_2 . Source and drain electrodes are patterned using electron

beam lithography in the form of an interdigitated set of electrodes with a systematic increase in the distance between each pair. The channel width, W , is kept fixed for all devices. Three different kinds of metallic electrodes (Au, Cr, Cu) were then deposited by electron beam evaporation followed by lift off. (25 nm of each, preceded by 2.5 nm of Ti adhesion layer; no Ti layer for Cr samples). Au electrodes were cleaned for one minute in a 1:1 solution of $\text{NH}_4\text{OH}:\text{H}_2\text{O}_2$ (30%), rinsed in de-ionized water, and exposed for about 1 min to oxygen plasma. The Cr samples were cleaned in the same manner followed by a last step dipping in a buffered HF solution for under 10 seconds. The HF is believed to etch the native SiO_2 oxide, exposing a fresh layer of dielectric. Cu electrodes on the other hand were only exposed to less than 25 seconds of O_2 plasma to clean the organic residue from the lift off. We found that Cu samples exposed to any cleaning procedure except for short O_2 plasma generally exhibited very poor transport properties.

The organic semiconductor is 98% regio-regular P3HT[19] a well studied material[20, 21, 22]. As received, RR-P3HT is dissolved in chloroform at a 0.02% weight concentration, passed through PTFE 0.02 micrometer filters, and solution cast onto the clean substrates, with the solvent allowed to evaporate in ambient conditions. The resulting films are tens of nanometers thick as determined by atomic force microscopy. The measurements are performed in vacuum ($\sim 10^{-6}$ Torr) in a variable-temperature probe station using a semiconductor parameter analyzer (HP4145B).

III. RESULTS AND DISCUSSION

The devices operate as standard p -type FETs in accumulation mode[23, 24]. With the source electrode grounded, the devices are measured in the shallow channel regime ($V_D < V_G$). Here we mainly concentrate on the experimental results of charge injection from Cr and Cu electrodes, as results on Au samples have been published elsewhere[5, 25].

A. Extracting contact current-voltage characteristics

Figures 1a and 1b show the transport characteristics ($I_D - V_D$) of a Cr device with $L = 25 \mu\text{m}$ and $W = 200 \mu\text{m}$ at $T = 300 \text{ K}$ and $T = 160 \text{ K}$ for a series of V_G s. The rise of current with voltage in the low V_D regime ($V_D < 3 \text{ V}$) is slightly super-quadratic. At higher drain voltages, the current becomes less nonlinear, at least in part due to saturation effects in the transistor. Our focus here is on low source-drain bias voltages. For comparison, $I_D - V_D$ plots for an Au sample with the same geometric parameters as above is also included in Figs. 1c and 1d.

The severe nonlinearity observed in the Cr data, in contrast to the linear injection from Au, is traditionally attributed to the existence of a Schottky energy bar-

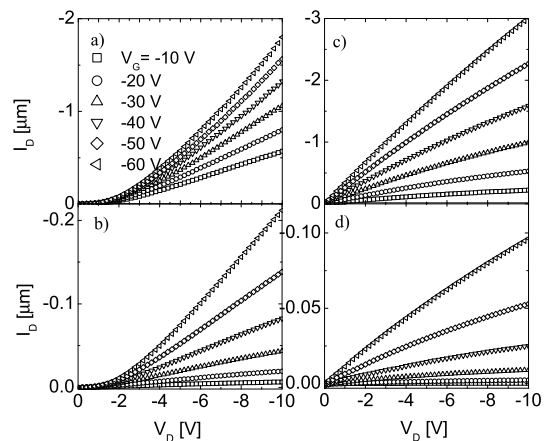


FIG. 1: (a) Transport characteristics ($I_D - V_D$) of a P3HT OFET with Cr source and drain electrodes, with $L = 25 \mu\text{m}$, $W = 200 \mu\text{m}$ at 300 K for several gate voltages. (b) Same device at 160 K. (c) Analogous plot for a sample with Au electrodes of the same geometry, at 300 K and (d) at 160 K.

rier, Δ , between the Fermi level of the metal and the HOMO of the polymer. It is generally accepted[16, 18] that the size of Δ alone determines the nature of transport in a device, *i.e.*, injection limited vs. bulk (or space charge limited) transport. In the space-charge case, most relevant when Δ is relatively small, the easily injected carriers significantly alter the local electric field from the average field imposed by the electrode potentials, and correspondingly limit the current. From individual $I_D - V_D$ traces, it can be difficult to distinguish between space charge effects and nonlinear contact injection because space charge limited transport is also significantly nonlinear[26]. One means of distinguishing the two is the detailed dependence of current on V and L [7, 18, 25]. A weak temperature dependence of current is also another signature of injection limited transport from metal into organic semiconductor[27].

The injection properties of the contact can be examined[7] by splitting the channel into two regimes of contact and the main channel. A voltage of V_C is dropped across the contact with the remaining $V_{\text{ch}} = V_D - V_C$ across the main channel. Using the charge control model[28], I_D can be written as:

$$I_D = WC\mu[V_G - V_T - V(x)]\frac{dV}{dx}, \quad (1)$$

where $V(x)$ is the potential in the channel at some position x , V_T is the threshold voltage, C is the capacitance per unit area of the gate dielectric, and μ is the intrinsic channel mobility. Integration of Eq. (1) from $x = 0$ to $L - d$ gives:

$$\frac{I_D}{WC\mu}(L - d) = (V_G - V_T)(V_D - V_C) - \frac{1}{2}(V_D^2 - V_C^2), \quad (2)$$

where V_C is dropped across d , a characteristic depletion length near the contacts. In this treatment, we

assume V_C to be entirely dropped across the injecting contact. Scanning potentiometry experiments in this material[8, 9, 10] have previously shown that, in systems with significant Δ , most of the potential drop due to contacts occurs at the source, where holes are injected into the channel.

Eq. (2) can be used to extract a value of V_C for any pair of (V_D, I_D) data, though there is no independent way of knowing the correct value of μ . With an array of devices, one can use the length dependence of I_D to address this difficulty. At a given T and V_G , a series of $I_D - V_D$ data is collected from devices with different channel lengths. The corresponding $I_D - V_C$ is calculated from Eq. (2) for all the different L . If the contact and channel transport properties in each device are identical, the correct value of μ would make all the different $I_D - V_C$ curves collapse onto one, since the injection characteristics of a particular OSC/metal interface should be unique and set by material properties and the (fixed) channel width and electrode geometry. This technique allows for the simultaneous extraction of μ and $I_D - V_C$. Since the average source-drain field in our devices is low ($< 10^3$ V/cm), no significant field dependence of μ is expected[7] or observed.

To confirm this method of extracting μ and $I_D - V_C$, we fabricated a series of devices (in a two-step lithography process) with *alternating* Au and Cr electrodes. The data is then taken twice for each device, once with the source electrode on Cr with the drain on Au and the second time *vice versa*. Fig. 2 shows a plot of extracted $I_D - V_C$ for injection from Cr and Au at $T = 240$ K and $V_G = -80$ V. We noticed that there is still a minute non-linearity present in data for Au at that is not present in all-Au devices. We believe that this is consistent with a small contact voltage at the drain, as was seen in the potentiometry profile of Cr/P3HT devices in Ref. [10]. The Au data in Fig. 2 have been shifted toward lower $|V_C|$ by 0.5 V to account for this. The value of μ that collapses the different length-dependent data for injection from Cr onto one $I_D - V_C$ curve is *identical* to that inferred from the length-dependence of the channel resistance when injection is from Au in the same devices. This demonstrates that this procedure of extracting $I_D - V_C$ is well-founded.

The mobilities in the Au/Cr devices are lower than those seen in all Au or all Cr source/drain samples (discussed below). We believe this to be due to inferior surface cleanliness of samples made in the two-step lithography technique. The contact resistance data for injection from Au agree *quantitatively* with the data observed in previous Au samples[5].

Fig. 3 shows a plot of measured $I_D - V_D$ and the current corrected for contact voltages, *i.e.* $I_D - V_{ch}$, for the all-Cr sample described above at $V_G = -60$ V. As seen from the plot, most of the total voltage is dropped across the contact, making these devices severely contact limited. For example, for a drain voltage of 2 V, $V_C/V_{ch} \sim 30$.

Fig. 4a shows the temperature dependence of μ ex-

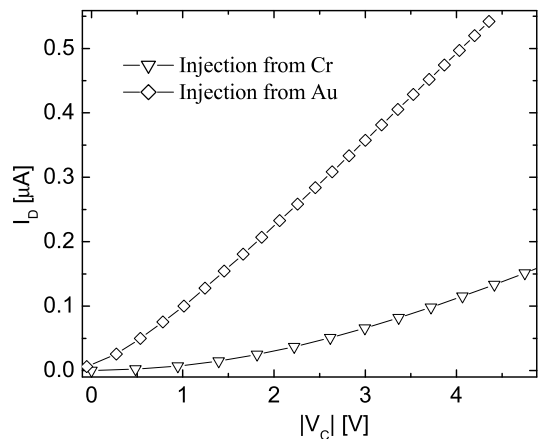


FIG. 2: Extracted $I_D - V_C$ for a series of devices of width $200 \mu\text{m}$ with alternating Cr and Au electrodes at 240 K and $V_G = -80$ V. Upper curve shows injection of holes from Au, while lower curve shows injection from Cr. Injection from Au is more linear and allows higher currents at lower voltages. The Au data have been shifted to lower $|V_C|$ by 0.5 V to account for a small contact voltage at the drain.

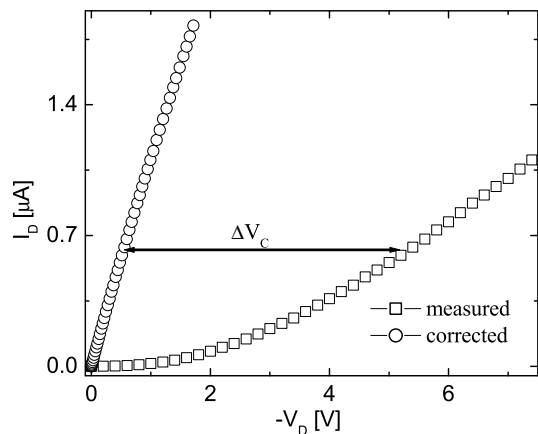


FIG. 3: Measured $I_D - V_D$, and the same data corrected for contact voltages (*i.e.* $I_D - V_{ch}$) for the Cr electrode device shown in Fig. 1, at 290 K and $V_G = -60$ V. The device is clearly quite contact limited.

tracted this way as a function of T^{-1} for a set of devices with all-Cr source/drain electrodes. The temperature dependence is well approximated as thermal activation consistent with simple hopping of carriers between localized states in the channel. The activation energies E_a for the mobility are quantitatively similar to those seen in all-Au devices[5]. The inset in Fig. 4a shows that the activation energies of the injected current (at $V_C = 1$ V) are *smaller* than E_a . In agreement with others' results[10, 17], this is *inconsistent* with the simple thermionic diffusion model of injection. As discussed in the next section, the hopping injection model predicts this weak temperature dependence.

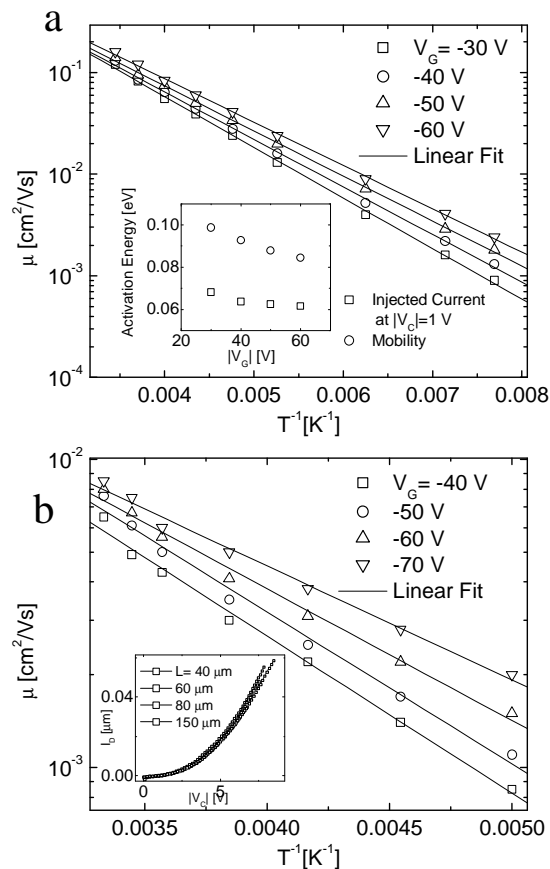


FIG. 4: Temperature dependence of the extracted channel mobility as a function of T^{-1} for sets of devices with (a) Cr and (b) Cu source and drain electrodes at several gate voltages. Inset in (a): Activation energies of the injected current and E_a as a function of V_G . Inset in (b): An example of “collapsed” $I_D - V_C$ data for devices of different values of L with Cu electrodes, $W = 400 \mu\text{m}$, 240 K , $V_G = -70 \text{ V}$.

A similar plot for the temperature dependence of channel mobility in a sample with Cu source/drain electrodes is shown in Fig. 4b. The values of μ in Cu devices are consistently lower than those seen in Cr or Au, though the activation energies are very similar. The reason for these lower mobilities remains unclear, since contact effects have been accounted for. However, it is commonly observed[10, 29] that the field effect mobility can be significantly different in nominally identically prepared samples. The values of contact resistivity, $R_c W$ are also higher in Cu devices. At a small $V_C \sim 1 \text{ V}$, $R_c W[\text{Cu}] \sim 3300 \text{ k}\Omega\text{-cm}$, while the corresponding value for Cr is $R_c W[\text{Cr}] \sim 125 \text{ k}\Omega\text{-cm}$. For devices with Au source/drain electrodes[5], $R_c W \sim 10 \text{ k}\Omega\text{-cm}$ was obtained. The increase in contact resistivity from Au to Cu is consistent with the increase in value of Δ as described below. The inset in Fig. 4b shows an example of a coalesced plot of $I_D - V_C$ for different values of L for the Cu sample at $T = 240 \text{ K}$ and $V_G = -70 \text{ V}$. A single

mobility value of $3.8 \times 10^{-3} \text{ cm}^2/\text{Vs}$ was used to obtain this collapse.

B. Interpretation and modeling

Having extracted nonlinear current-voltage characteristics for the injecting contacts, we analyze the resulting data in terms of a particular model of injection into disordered polymer semiconductors. As mentioned earlier, the diffusion thermionic models are insufficient to account for the weak temperature dependence of the observed injected current. The analytic treatment by Arkhipov *et al.*[18] of charge injection from a metallic electrode into a random hopping system has been shown[17, 27] to consistently explain the field and temperature dependence of charge injection in organic Schottky diode-like structures. In this picture, the weak temperature dependence of the injection current is a consequence of a Gaussian distribution of states[30]. Therefore the injection process is easier at lower temperatures, leading to a weaker temperature dependence of the current. Here we apply Arkhipov results to our charge injection data in OFETs and show that this treatment, with reasonable parameters, is consistent with the measured data.

Key to this analysis is the conclusion[10, 31] that a small depletion region forms in the vicinity of the contacts, and that V_C is dropped across this region at the injecting contact. We note that the values of V_C can be as large as a few Volts. Establishing the distance scale, d , relevant to converting this into the electric field at the contact is nontrivial, though reasonable bounds may be placed on this parameter. The resolution of existing scanning potentiometry data in similar OFET structures[9, 10] establishes that d cannot exceed $\sim 400 \text{ nm}$. Furthermore, the lack of breakdown or irreversible device damage implies that the injecting field must be below the breakdown field of the OSC, so that d must be larger than $\sim 10 \text{ nm}$. After presenting the analysis of the $I_D - V_C$ data, we return to this issue below.

In this 1d model[18], the transport of carriers takes place in a hopping system of Gaussian energy distribution in close contact with the metallic electrode. This density of states (DOS) is given by:

$$g(E) = \frac{N_t}{\sqrt{2\pi}\sigma} \exp\left(-\frac{E^2}{2\sigma^2}\right), \quad (3)$$

where N_t is the total spatial density of localized states, with σ as the variance of the gaussian distribution centered about $E = 0$. The emphasis is placed on the primary injection event where a carrier from the metal is injected into a localized state a distance $x_0 > a$ from the interface, where a is the intersite hopping distance. The potential of this carrier at any distance x from the interface is given by

$$U(x, E) = \Delta - \frac{e^2}{16\pi\epsilon_0\epsilon x} - eF_0x + E, \quad (4)$$

where Δ is the energy difference between the Fermi level of the metal and the center of DOS in the semiconductor, F_0 is the external field at the contact, e is the elementary charge, and ϵ is the relative dielectric constant of the polymer. Once a carrier is injected into a localized state in the polymer, it can either go back to the metal due to the attractive image potential, or escape with a finite probability to diffuse into the bulk. The escape probability can be solved using the 1d Onsager problem as outlined in detail in Ref. [18]. The final result predicts the injection current density as follows:

$$J_{\text{inj}} = e\nu \left(\int_a^\infty dx \exp \left[-\frac{e}{k_B T} \left(F_0 x + \frac{e}{16\pi\epsilon_0\epsilon x} \right) \right] \right)^{-1} \times \int_a^\infty dx_0 \exp(2\gamma x_0) \int_a^{x_0} dx \exp \left[-\frac{e}{k_B T} \left(F_0 x + \frac{e}{16\pi\epsilon_0\epsilon x} \right) \right] \times \int_{-\infty}^\infty dE' \text{Bol}(E') g[U(x_0) - E']. \quad (5)$$

Here, ν is the attempt-to-jump frequency, T is the temperature, γ is inverse localization length, and the Boltzmann function $\text{Bol}(E)$ is defined as:

$$\begin{aligned} \text{Bol}(E) &= \exp(-E/k_B T), E > 0, \\ &= 1, E < 0. \end{aligned} \quad (6)$$

To apply this model, we first need to fix the parameters σ , a , and γ . It is possible to extract σ from a model of carrier transport in a disordered Gaussian density of states[32, 33] by plotting $\ln(\mu_0)$ vs. T^{-2} , where μ_0 is the value of the zero-field mobility. We note that our data appear to be better described as exponential in T^{-1} rather than T^{-2} ; nonetheless this procedure provides an estimate for a value of σ . Calculation of the values of a and γ [32] can be difficult, as one has to use the strong field dependence of mobility. As mentioned earlier, our data are acquired in a low enough source-drain average field that no field-dependence of μ may be inferred. Therefore, we chose a and γ consistent with reported values in literature[32] or previous experiments[25]. We note that changing a or γ over a reasonable range mainly affects the overall prefactor of the current (as described below), without significantly altering the shapes of the predicted curves.

With σ , a , and γ held fixed, the only parameters that can be adjusted to fit Eq. (5) to a plot of data are Δ , a prefactor $K \equiv A\nu N_T$ (where A is an effective injection area), and d , where $F_0 = V_C/d$. We observed, as discussed in detail in Ref. [18], that the nonlinearity in a plot of $I_D - V_C$ is mainly controlled by the value of Δ and the strength of the electric field. At $F_0 \sim 5 \times 10^7$ V/m or higher, the plots are severely nonlinear and the temperature dependence of the current would be extremely weak. At lower fields, the nonlinearity is less severe and the temperature dependence is stronger. Therefore, the value of d is paramount, and constrained as described above.

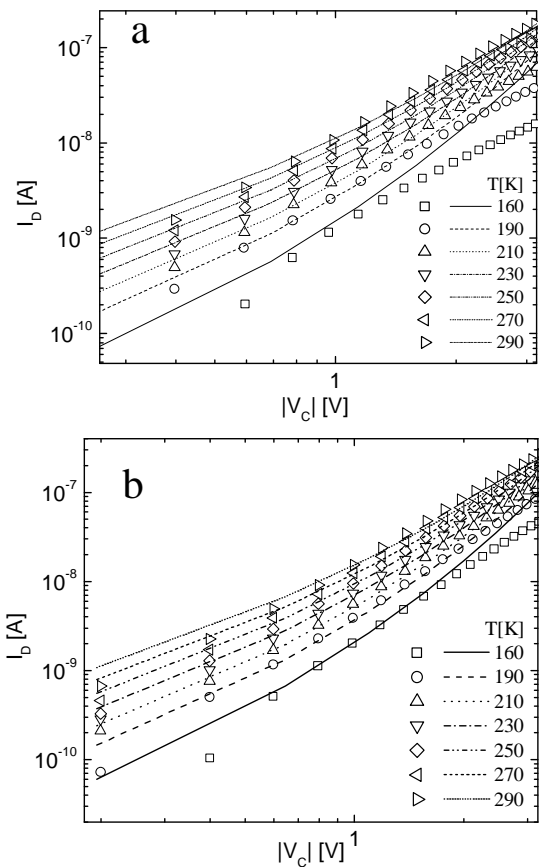


FIG. 5: $I_D - V_C$ data from a set of Cr electrode devices, together with curves from the model of Eq. (5) at gate voltages (a) -30 V, and (b) -60 V.

Having expected $\Delta \sim 0.3$ eV, we find that d cannot be below 100 nm within this model; the resulting large values of injecting field F_0 would yield temperature and field dependences inconsistent with those observed. Table I summarizes the parameters used to model the injection data for both all-Cr and all-Cu sets of devices. Figures 5a and b show plots of $I_D - V_C$ and the corresponding numerical integration of Eq. (5) using parameters given in Table I (with an appropriate value of prefactor K) for injection from Cr over a representative range of temperature for gate voltages -30 V and -60 V. Fig. 6 shows the temperature dependence of the injected current in low V_C regime and the Arkhipov fit to the data. Notice that the predicted temperature dependence in the diffusion thermionic model is much stronger than the Arkhipov model if the same $\Delta = 0.23$ eV is used. Fig. 7 shows a plot of $I_D - V_C$ for a Cu sample at $V_G = -60$ V. The fit to the data is valid only in the low V_C regime as saturation effects in the transistor start to affect $I_D - V_D$ data at large V_D . Note that the procedure outlined above to extract the $I_D - V_C$ data assumes that devices are firmly in the gradual channel limit, with no saturation effects. Also, the effects of leakage currents to the gate electrode in the immediate vicinity of $V_C = 0$ at low temperatures

TABLE I: Parameters used to model the $I_D - V_C$ data of this study within the charge injection treatment of Ref. [18] for all T . The relative dielectric constant ϵ of the polymer was assumed to be 3. At each gate voltage a single numerical prefactor was the only necessary adjustment.

Contact	σ	a	γ	Δ	d
metal	[eV]	[nm]	[nm ⁻¹]	[eV]	[nm]
Cr	0.046	1.6	4.35	0.23	150
Cu	0.046	1.6	4.35	0.31	230

can be seen in Figs. 5 and 7.

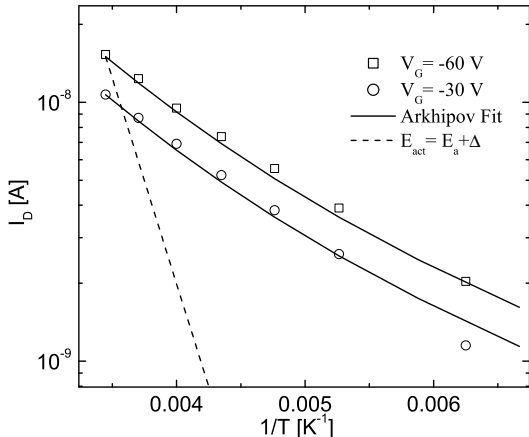


FIG. 6: Temperature dependence of the injected current for Cr electrodes at low V_C , with Eq. (5) fits to the data. The dashed line shows the predicted T dependence of the thermionic diffusion model for the same value of Δ .

N_t is the only gate-dependent parameter in this model. The parameters listed in Table I are kept fixed for all temperatures and all gate voltages. Since the prefactor in Eq. (5) is the product $A\nu N_t$, it is therefore not possible to determine an exact value for just N_t . For a cross-sectional area of injection of $A \sim 25 \text{ nm} \times 2 \times 10^5 \text{ nm}$ and $\nu \sim 10^{13} \text{ s}^{-1}$, we find $N_t \sim 1.1 \times 10^{22} \text{ cm}^{-3}$ for $V_G = -60 \text{ V}$ and $N_t \sim 8.3 \times 10^{21} \text{ cm}^{-3}$ for $V_G = -30 \text{ V}$. These values are consistent with other experiments[17, 27].

Table I shows that the obtained injection barrier height for copper is about 80 meV higher than that for Cr. This difference in the barrier energy is not unreasonable, and may be attributed[10] to an interfacial dipole layer at the interface changing Δ by a small amount. *In-situ* ultraviolet photoemission spectroscopy measurements would be well-suited to testing this hypothesis[34, 35, 36]. The higher injection barrier for copper is consistent with the observed higher contact resistivity and lower overall currents observed in Cu.

The length of the presumed depletion region is also a bit higher in Cu samples (by $\sim 80 \text{ nm}$), though it does not necessarily reveal why the mobility is lower in these devices. The origin of these depletion regions in the vicinity of the contacts is not understood in detail. Recent

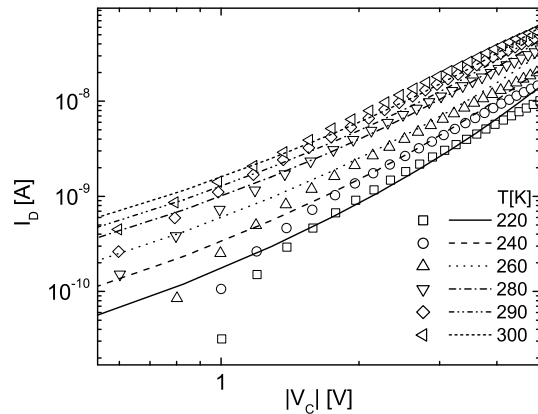


FIG. 7: $I_D - V_C$ for devices with Cu electrodes ($W = 400 \text{ nm}$) at $V_G = -60 \text{ V}$ over a representative temperature range, together with results from Eq. (5) and the parameters of Table I.

2d electrostatic modeling[31] of OFETs has shown that the effect of significant energy barriers at the injecting electrode is formation of regions of low carrier concentration (and mobility) near the contacts. These studies place the extent of these regions at about 100 nm from the contact, depending on V_G . Another possible origin for regions of reduced mobility near metal contacts with significant barriers is charge transfer and band bending near the interface. Since conduction in these materials can be treated as percolative variable range hopping[37], μ is a natural function of the density of available hopping sites. The occupation of those sites can be strongly modified by interfacial charge transfer between the metal and the OSC. Improved local probes (nm-resolution scanning potentiometry, cross-sectional scanning tunneling microscopy) would be extremely useful in better understanding these depletion regions.

V. CONCLUSIONS

Transport properties of a series of organic field effect transistors with P3HT as the active polymer layer and Cr, Cu and Au as the source/drain electrodes were examined over a temperature range. The contact current-voltage characteristics for these devices were extracted from the length dependence of conductance, with the assumption that the injection barrier primarily applies to holes being injected from the source. This procedure was checked for consistency using devices with electrodes of alternating metal composition. The data confirm that the weak temperature dependence of the injected current cannot be simply explained using the general diffusion-thermionic emission models. With reasonable values of parameters, a more sophisticated model of hopping injection into a disordered density of localized states, with emphasis on the primary injection event, is consistent with the field and the temperature dependence of the

data over a broad range of temperatures and gate voltages.

VI. ACKNOWLEDGMENT

The authors gratefully acknowledge the support of the Robert A. Welch Foundation and the Research Corpora-

tion.

-
- [1] C.D. Dimitrakopoulos and D.J. Mastro. IBM J. Res. Dev. **45** 11 (2001).
- [2] J.C. Scott, J. Vac. Sci. Tech. A **21**, 521 (2003).
- [3] H. Klauk *et al.* Sol.-State Elect. **47**, 297 (2003).
- [4] P.V. Necludiov, M.S. Shur, D.J. Gundlach, and T.N. Jackson. Sol.-State Elect. **47**, 259 (2003).
- [5] B.H. Hamadani and D. Natelson. Appl. Phys. Lett. **84**, 443 (2004).
- [6] G. Horowitz, R. Hajlaoui, D. Fichou, and A. El Kassmi. J. Appl. Phys. **85**, 3202 (1999).
- [7] R.A. Street and A. Salleo. Appl. Phys. Lett. **81**, 2887 (2002).
- [8] K. Seshadri and C.D. Frisbie. Appl. Phys. Lett. **78**, 993 (2001).
- [9] L. Bürgi, H. Sirringhaus, and R.H. Friend. Appl. Phys. Lett. **80**, 2913 (2002).
- [10] L. Bürgi, T.J. Richards, R.H. Friend, and H. Sirringhaus. J. Appl. Phys. **94**, 6129 (2003).
- [11] J. Zaumseil, K.W. Baldwin, and J.A. Rogers. J. Appl. Phys. **93**, 6117 (2003).
- [12] E.J. Meijer, G.H. Gelinck, E. van Veenendaal, B.-H. Huisman, D.M. de Leeuw, and T.M. Klapwijk. Appl. Phys. Lett. **82**, 4576 (2003).
- [13] G.B. Blanchet, C.R. Fincher, and M. Lefenfeld. Appl. Phys. Lett. **84**, 296 (2004).
- [14] J.C. Scott and G.G. Malliaras. Chem. Phys. Lett. **299**, 115 (1999).
- [15] Y. Shen, M.W. Klein, D.B. Jacobs, J.C. Scott, and G.G. Malliaras. Phys. Rev. Lett. **86**, 3867 (2001).
- [16] Z. Chiguvare, J. Parisi, and V. Dyakonov. J. Appl. Phys. **94**, 2440 (2003).
- [17] T. van Woudenberg, P.W.M. Blom, M.C.J.M. Vissenberg, and J.N. Huiberts. Appl. Phys. Lett. **79** 1697 (2001).
- [18] V.I. Arkhipov, E.V. Emelianova, Y.H. Tak, and H. Bässler. J. Appl. Phys. **84** 848 (1998).
- [19] Sigma-Aldrich Inc., St. Louis, MO.
- [20] Z. Bao, A. Dodabalapur, and A.J. Lovinger. Appl. Phys. Lett. **69** 4108 (1996).
- [21] H. Sirringhaus, N. Tessler, and R.H. Friend. Science **280** 1741 (1998).
- [22] H. Sirringhaus, P. J. Brown, R. H. Friend, M. M. Nielsen, K. Bechgaard, B. M. W. Langveld-Voss, A. J. H. Spiering, R. A. J. Janssen, E. W. Meijer, P. Herwig, and D. M. de Leeuw. Nature **401** 685 (1999).
- [23] A.N. Aleshin, H. Sandberg, and H. Stubb, Synth. Met. **121**, 1449 (2001).
- [24] E.J. Meijer, C. Tanase, P.W.M. Blom, E. van Veenendaal, B.-H. Huisman, D.M. de Leeuw, and T. M. Klapwijk, Appl. Phys. Lett. **80**, 3838 (2002).
- [25] B.H. Hamadani and D. Natelson, J. Appl. Phys. **95**, 1227 (2004).
- [26] P. N. Murgatroyd, J. Phys. D **3**, 151 (1970).
- [27] J. Reynaert, V. I. Arkhipov, G. Borghs, and P. Heremans, Appl. Phys. Lett. **85**, 603 (2004).
- [28] M. Shur, *Physics of Semiconductor Devices* (Prentice-Hall, Inc., 1990).
- [29] S.F. Nelson, Y.-Y. Lin, D.J. Gundlach, and T.N. Jackson, Appl. Phys. Lett. **72**, 1854 (1998).
- [30] V.I. Arkhipov, U. Wolf and H. Bassler, Phys. Rev. B. **59**, 7514 (1999).
- [31] T. Li, P.P. Ruden, I.H. Campbell, and D.L. Smith, J. Appl. Phys. **93**, 4017 (2003).
- [32] H.C.F. Martens, P.W.M. Blom and H.F.M. Schoo, Phys. Rev. B. **61**, 7489 (2000).
- [33] H. Bassler, Phys. Status Solidi B. **175**, 15 (1993).
- [34] I.G. Hill, A. Rajagopal, A. Kahn, and Y. Hu. Appl. Phys. Lett. **73**, 662 (1998).
- [35] X. Crispin, V. Geskin, A. Crispin, J. Comil, R. Lazzaroni, W.R. Salaneck, and J.-L. Brédas. J. Am. Chem. Soc. **124**, 8131 (2002).
- [36] N. Koch, A. Kahn, J. Ghijsen, J.-J. Pireaux, J. Schwartz, R.L. Johnson, and A. Eischner. Appl. Phys. Lett. **82**, 70 (2003).
- [37] M.C.J.M. Vissenberg and M. Matters. Phys. Rev. B **57**, 12964 (1998).